Ultrasonics Sonochemistry 84 (2022) 105973

Contents lists available at ScienceDirect

Ultrasonics Sonochemistry

journal homepage: www.elsevier.com/locate/ultson

New insights into the ultrasound impact on covalent reactions of myofibrillar protein

Jiahui Chen [a], Xing Chen [b], Guanghong Zhou [a], Xinglian Xu [a,*]

[a] Key Laboratory of Meat Processing, Ministry of Agriculture, Key Lab of Meat Processing and Quality Control, Ministry of Education, Jiangsu Collaborative Innovation Center of Meat Production and Processing, College of Food Science and Technology, Nanjing Agricultural University, Nanjing 210095, China
[b] State Key Laboratory of Food Science and Technology, School of Food Science and Technology, Jiangnan University, Wuxi, Jiangsu 214122, China

ARTICLE INFO

Keywords:
Myofibrillar protein
Ultrasound treatment
Gallic acid
Covalent reactions
Acoustic cavitation
Rheological properties

ABSTRACT

In this work, two different covalent reactions, namely, alkaline reaction and free radical oxidation, were selected to compare the difference in the strengthening effects of ultrasound treatment (UDT). The grafting effects were verified by protein electrophoresis and bound gallic acid (GA) assay. Furthermore, non-covalent interactions between myofibrillar protein (MPN) aggregates were destroyed by UDT, as proved by the lower particle sizes and higher ζ-potential. Comparatively, the results from tertiary structure index and circular dichroism revealed UDT-assisted free radical oxidation could lead to better conjugates with greater structural properties. The atomic force microscope (AFME) and protein flexibility showed that MPNs appeared to display as irregular spherical particles after alkaline reaction, however, maintained fibrous structure during the free radical oxidation. Consequently, the combination of UDT and free radical oxidation were more effectively for strengthening the influence of acoustic cavitation on MPNs, of which mechanism was the changes in viscosity properties, microstructure and acoustic cavitation radicals.

1. Introduction

Developing high-quality protein products from meat as nutritional supplements for the special populations has been the goal of food researchers in recent years [1]. Myofibrillar proteins (MPNs), the most abundant protein in meat, have been considered as a special choice for many years. In virtue of their unique structure and superior biological digestibility, researchers are eager to apply MPNs as building blocks for exploiting brand-new protein products. Moreover, a large number of novel strategies have been tried to ameliorate the water solubility, dispersion [2] and thermal stability [3] of MPN system. These studies interpret the possibilities of developing MPN as nutrient supplements from different perspectives. However, due to the lack of functionality, such products seem to be difficult to further attract consumers. At this time, polyphenol modification of MPN is essential for improving its insufficient functionality.

Benefiting from its excellent antioxidant properties and pharmacological actions, gallic acid (GA) is often selected for the modification of protein systems to make up for their lack of functional properties. As reported, GA exhibited good anti-inflammatory [4], anti-carcinogenic [5] and anti-obesity properties [6]. Additionally, GA could form intermediate object to react with active sites, including amino group ($-NH_2$) and/or sulfhydryl group (–SH), in MPN to change the structural and functional properties of protein.

Although GA modification exhibited excellent ability in improving various properties of MPNs, unfavorable precipitation may be formed by protein crosslinking. Moreover, traditional covalent grafting is time-consuming and inefficient. Hence, several studies are seeking for creative approaches to replace the traditional ones. Ultrasound treatment (UDT) in combination with GA modification is assumed to be an interesting method to improve the undesirable characteristics of MPNs [7]. It has long been considered that the critical advantages of UDT-assisted modification are the improvement of efficiency and ease of operation. As reported [6,8], UDT could directly trigger the generation of OH· in the Japanese seerfish MPN solution, contributing to the covalent reaction between MPN and GA. Moreover, another study [9] also confirmed that additional hydroxyl radicals (OH·) produced by UDT directly enhanced the yield of (−)-epicatechin gallate-MPN complex. In this regard, cavitation bubbles can be produced rapidly during UDT, cutting the solvent molecules to generate OH· at the moment of their periodic rupture ($H_2O \rightarrow OH\cdot + H\cdot$). In comparison to free radicals induced by the conventional ascorbic acid system, UDT-triggered radicals are more

* Corresponding author.
E-mail address: xlxus@njau.edu.cn (X. Xu).

https://doi.org/10.1016/j.ultsonch.2022.105973
Received 9 January 2022; Received in revised form 18 February 2022; Accepted 1 March 2022
Available online 3 March 2022

controllable. However, radicals provided by UDT are highly transient, and their yields are closely related to the environment [10]. In addition, the protein structure and system status under different covalent reactions may also affect the strength of cavitation bubbles. Notably, an UDT-induced "stress response" of myosin during the acoustic cavitation was also related to the action of cavitation bubbles [11]. Therefore, it is of great importance to investigate the difference in the strengthening effects of UDT for different covalent reactions.

In this study, alkaline reaction and free radical oxidation were selected for covalent reactions of GA. The objective of this work was to compare the difference in the strengthening effects of UDT for different reactions. Covalent structure and conjugate efficiency were firstly evaluated after different modifications. Then, structural properties of MPN after various modifications were also assessed. In addition, viscosity properties, microstructure, MPN flexibility and antioxidant properties were compared to study the difference of functional properties caused by the UDT. This study contributed to seek the best synergistic action to maximize process efficiency.

2. Materials and methods

2.1. Materials and reagents

Fresh chicken breast (white feathered chicken, ~9 pieces, $pH_{24h} \approx 6.0$, $L^*_{24h} \approx 52$, 4 °C) was purchased from Jiangsu Sushi Meat Co., Ltd. (Nanjing, Jiangsu). Chicken breast meat was obtained from broilers after being slaughtered according to the industrial standards. GA (off-white powder, molecular weight: 170.12, purity ≥ 98%, origin: plant), 2,2-diphenyl-1-picrylhydrazyl (DPPH), 3-ethylbenzothiazoline-6-sulfonic acids (ABTS), and vitamin E (Trolox) and other reagents (analytical grade) were provided by Solarbio Technology Co., Ltd. (Beijing, China).

2.2. Isolation of MPNs

The isolation of MPNs was conducted based on the procedure of a previous study [9]. Extracted solutions (1440 mL, 0.1 mol/L KCl, 2 mmol/L EGTA, 1 mmol/L $MgCl_2$, pH 7.0) were prepared two days in advance. Briefly, selected chicken breast was minced (3000 rpm, 30 s, 4 °C) into meat slurry. Subsequently, these slurries (120 mL) were washed with the extracted solution (480 mL) for the homogenization (8000 rpm, 10 s, 3 times). Obtained slurries were then subjected to a suitable centrifugation (9.5 min, 4 °C, 4100 rpm). After carefully collection, the same procedure was conducted in triplicate. Then, obtained precipitations (120 mL) were also mixed again with the NaCl solution (0.1 mol/L, 480 mL) for the homogenization (8000 rpm, 10 s, 3 times). These slurries were subjected to a suitable centrifugation (9.5 min, 4 °C, 4100 rpm). These treatments were also performed in triplicate to achieve the final MPN samples.

2.3. Preparation of MPN samples

To investigate the strengthening effects of UDT on different covalent modifications, MPN samples were subjected to 5 different treatments: CON: without GA and UDT; A1: without UDT, but GA was incorporated for the alkaline reaction; A2: GA was incorporated for the alkaline reaction during UDT; F1: without UDT, but GA was incorporated for the free radical reaction; F2: GA was incorporated for the free radical reaction during UDT.

Briefly, different GAs (15 μmol/g MPN) were incorporated into the MPN samples (30 g/L) to obtain the mixture (50 mL) for the homogenization (6500 rpm, 10 s) [9]. For the A1 group, the mixture containing GA and MPN was adjusted to a pH of 9.0. Then, the alkaline reaction was activated during the stirring process (350 rpm, 30 min). Afterwards, the pH of experimental mixture was adjusted back to 7.0. To note, the steps of the alkaline reaction in the A2 group were the same as those in the A1 group. However, UDT (pulsed UDT, power: 350 ± 20 W/L, actual processing time: 6 min, temperature: 4 °C, diameter of the probe: 2.0 cm) was performed during the stirring. For the F1 group, 0.125 g of ascorbic acid and 0.5 mL of hydrogen peroxide (10 mol/L) were added to 50 mL of the MPN solution. Thereafter, the GA was incorporated into the mixture under stirring (350 rpm, 30 min) for the free radical reaction. It should be noted that the steps of the free radical reaction in the F2 group were the same as those in the F1 group. However, UDT was performed during the stirring. All unreacted GA was removed (24 h) via using dialysis at 4 °C, which can be verified through Folin-Ciocalteu method.

2.4. Verification of covalent structure

Covalent structure of prepared MPNs (CON, A1, A2, F1 and F2) was verified by protein gel electrophoresis. Briefly, 80 μL of different MPN samples (CON, A1, A2, F1 and F2, 1.5 g/L) were thoroughly mixed with 20 μL of 5 × loading buffers (125 mmol/L Tris, pH 6.80, 200 mmol/L 2-mercaptoethanol, 4% sodium dodecyl sulfate). Thereafter, 5 μL of mixed samples containing different MPNs were vortexed for 3 s (3 times). The uniform mixtures were loaded into the fixed well for the structural verification at a recognized voltage (90 V). The premade dye and deintegration solution was used for the incubation (2 h) of the strips to facilitate the scanning of the obtained gels.

2.5. Bound GA assay

The contents of GA bound to MPN after different modifications were evaluated through traditional Folin-Ciocalteu method [12]. A mixture (9 mL) containing 1.5 mL of different MPN solutions after various modifications and 7.5 mL of purchased Folin-Ciocalteu reagent (0.25 mol/L) was put in the cold storage (5 min, 4 °C) for the reaction. Then, 6 mL of prepared Na_2CO_3 (7.5%, w/v) solution was thoroughly mixed with previous solution for 120 min. After centrifugation at 6000 rpm (4 °C) for 15 min, 200 μL of the supernatant was transferred for the measurement of the absorbance (760 nm). The contents of GA bound to different MPNs were calculated by using the standard curves of GA. Final results were expressed as μmol GA equivalent per g copolymer. The conjugate efficiency was also calculated as follows:

$$Conjugate\ efficiency = \frac{measured\ GA\ contents}{total\ GA} \times 100\% \quad (1)$$

2.6. Measurements of free radical contents

2.6.1. Terephthalic acid dosimetry

Terephthalic acid tends to be oxidized by the OH· [13] to form 2-hydroxyterephthalic acid. The free radical contents of MPN samples was also evaluated through the contents of formed 2-hydroxyterephthalic acid in the solution. Briefly, terephthalate solution (2 mmol/L terephthalic acid, 25 mmol/L NaOH, 2.5 mmol/L phosphate buffer) was added to samples before UDT. Then, the free radical contents were assessed through the fluorescence intensity of final samples (excitation wavelength: 310 nm, emission wavelength: 400–500 nm) after UDT.

2.6.2. Phenanthroline dosimetry

Phenanthroline-Fe^{2+} tends to be oxidized by the OH· in the solution to form Phenanthroline-Fe^{3+}. The free radical contents of MPN samples was also evaluated through the contents of formed Phenanthroline-Fe^{3+} in the solution. Briefly, phenanthroline solution (0.75 mmol/L 1,10-phenanthroline, 0.75 mmol/L ferrous sulfate) was added to samples before UDT. Then, the free radical contents were assessed through the absorbance value (536 nm) of final samples after UDT.

2.6.3. Crystal violet dosimetry

The addition reaction of C = C in crystal violet with OH· leads to the changes of the solution color. The free radical contents of MPN samples

was also evaluated through the contents of changed crystal violet in the solution. Briefly, crystal violet solution (0.1 mmol/L) was added to samples before UDT. Then, the free radical contents were assessed through the absorbance value (580 nm) of final samples after UDT.

2.7. Particle sizes and ζ-potential

The particle sizes [14] of prepared MPNs (CON, A1, A2, F1 and F2) were determined through using the principle of light scattering (Mastersizer 3000, Malvern Instruments Ltd., UK). The MPN samples were diluted to the set concentration (1 mg/mL). Then, 2 mL of prepared proteins were added to the sample box. The particle size of MPNs and their corresponding particle size distribution can be obtained directly by the instrument. ζ-potential of prepared MPNs (CON, A1, A2, F1 and F2) were evaluated through another instrument (Nano ZS 90, Malvern Instruments Ltd., UK). Briefly, 0.5 mL of prepared proteins (1 mg/mL) were added to the sample box. Also, ζ-potential of these MPN samples was calculated based on the frequency shifting of the light scattered by the charged protein. Final results were provided by the instrument.

2.8. Surface hydrophobicity (SEH) and sulfhydryl content (SLT)

The SEH [15] of prepared MPNs (CON, A1, A2, F1 and F2) was measured through hydrophobic probe. Briefly, MPN samples (8 mL, 0.5–5.0 mg/mL) and 8-anilino-1-naphthalenesulfonic acid (40 μL) was mixed to obtain the stable liquid. Then, the fluorescence intensity of MPN was detected (4 °C) after the reaction for 20 min (excitation: 375 nm, emission: 470 nm). To note, experimental SEH was assessed via using the slope of measured fluorescence intensity versus MPN concentrations (0.5–5.0 mg/mL).

The SLT of prepared MPNs (CON, A1, A2, F1 and F2) was measured through Ellman's reagent (5,5′-Dithiobis-(2-nitrobenzoic acid)). Briefly, MPN samples (2 mL, 1 mg/mL) and experimental Ellman's reagent (50 μL) was thoroughly mixed to achieve a reaction (4 °C) for 25 min. To note, experimental SLT was assessed via using the absorbance of final MPN samples (412 nm) [9].

2.9. Secondary structure

The secondary structure of fresh MPN samples (CON, A1, A2, F1 and F2) were evaluated through the circular dichroism (Jasco, Tokyo, Japan) [9]. In brief, MPN solutions (1.5 mL) after various treatments (CON, A1, A2, F1 and F2) were transferred to a quartz tube (1 cm). Then, the spectral information was collected at 5 nm/s (190–260 nm, 4 °C). The final secondary structure were carried out through using their inner program (Secondary Structure Estimation). All measurements were performed in triplicate.

2.10. Turbidity

The turbidity of MPN samples (CON, A1, A2, F1 and F2) was evaluated through the Microplate Reader (Tecan, Austria). To be specific, MPN samples were mixed with phosphate buffer (50 mM) to achieve a suitable concentration (1 mg/mL). Subsequently, experimental turbidity was assessed via using the absorbance of final MPN samples (660 nm).

2.11. Viscosity properties

The viscosity properties of fresh MPN samples (CON, A1, A2, F1 and F2) were conducted through the changes of shear rates (Anton Paar, Austria). Briefly, MPNs were firstly placed on the rheometer for 60 s. Then, the shear rate range (0.1 to 100 s^{-1}) was selected for the measurements (4 ℃) of viscosity properties. In addition, changes in apparent viscosity under high-speed (400 s^{-1}) and low-speed shear rate (1 s^{-1}) were also measured. In this regard, the shear rate was constant at 1 s^{-1} for 50 s. Thereafter, the shear rate rapidly increased to 400 s^{-1}, and remained constant at 400 s^{-1} for 50 s. Ultimately, the shear rate quickly decreased to 1 s^{-1} again, and remained constant at 1 s^{-1} for the next 50 s.

To evaluate the viscosity properties of MPNs comprehensively, some proposed models (e.g. Power law model and Carreau model) were applied in this work. Power law model [9] was fitted according to the following formula:.

$$\eta = k \times \gamma^{n-1} \tag{2}$$

Where η is apparent viscosity of measured MPNs, γ and k are pre-set shear rates and consistency parameter of MPNs, respectively. n is fitted non-newtonian parameter.

Carreau model [16] was fitted according to the following formula:

$$\eta = \eta_0 \left[1 + (\lambda\gamma)^2\right]^{\frac{a-1}{2}} \tag{3}$$

Where η_0 and λ are zero shear viscosity and relaxation coefficient of MPN samples, respectively. a is fitted shear index.

2.12. Antioxidant properties

2.12.1. DPPH scavenging activities

The DPPH scavenging activities (%) of fresh MPN-GA samples (CON, A1, A2, F1 and F2) were evaluated via using the methods of Zhang et al. [17]. To be specific, fresh MPN-GAs (2.0 mL, 0, 0.01, 0.05, 0.25, 1 and 4 mg/mL), DPPH ethanol solution (0.8 mL, 0.4 mM) were incorporated into the water (4.0 mL). Then, obtained mixtures were centrifuged (6000 rpm, 15 min) after the reaction for 30 min (4 °C, in the darkness). Final DPPH scavenging activities were assessed through the transformation of measured absorbance (517 nm).

2.12.2. ABTS scavenging activities

The ABTS scavenging activities (%) of fresh MPN-GA samples (CON, A1, A2, F1 and F2) were evaluated via using the methods of Yıldırım et al. [18]. To be specific, ABTS (25 mg) was added to the potassium persulfate (6.5 mL, 2.45 mmol/L) solution. Subsequently, the prepared ABTS solution was stored (14 h) at a constant temperature (25 ℃). The maintenance of the absorbance (734 nm, 0.70 ± 0.10) was confirmed before the experiments. Then, fresh MPN-GAs (1.0 mL, 1 mg/mL) and the prepared ABTS (3 mL) solution were subjected to an incubation process (60 min). Final ABTS scavenging activities were evaluated through the transformation of measured absorbance (734 nm). Moreover, these changes were converted to μmol Trolox equivalents (TE) per g of experimental samples (MPN-GAs).

2.12.3. Ion reduction capacities

The ion (III) reduction capacities (%) of fresh MPN-GA samples (CON, A1, A2, F1 and F2) were evaluated via using the strategy of Xu et al. [19]. Briefly, the mixture containing 2 mL of fresh MPN-GAs (1 mg/mL), 5 mL of buffer solution (phosphate, 0.2 mol/L) and 5 mL of potassium ferricyanide (1%, w/v) were mixed (51 °C) for 21 min. Thereafter, 5 mL of prepared trichloroacetic acid (10%, w/v) was incorporated to the mixed system immediately. Then, obtained solutions were centrifuged (14 min, 3500 rpm). Final ion (III) reduction capacities were evaluated through the transformation of measured absorbance (700 nm) of the mixture containing the supernatant (1.25 mL), distilled water (0.25 mL) and ferric chloride (0.5 mL, 0.1%, w/v). Moreover, these changes were converted to μmol Trolox equivalents (TE) per g of experimental samples (MPN-GAs).

2.13. Microstructure

The microstructure of different groups (CON, A1, A2, F1 and F2) was evaluated through atomic force microscope (AFME). For AFME, the fresh MPN sample was dripped onto a mica sheet. Subsequently, the silicon cantilever operated in acoustic percussion mode (75 kHz, 0.4 N/

m) to facilitate image formation. Final AFME images were analyzed through Nanoscope Analysis software. Cross-sections and Rq are the uniformity and roughness average of the system, respectively, which were directly given by the software.

2.14. MPN flexibility

The MPN flexibility of different groups (CON, A1, A2, F1 and F2) was measured via using the hydrolysis of trypsin [20]. Briefly, fresh mixtures containing trypsin (0.5 mL, 1000 U/mL, 1 mg/mL, pH 8.0) and prepared MPN (8 mL, 1 mg/mL, pH 8.0) were heated in a water bath at 38 °C (450 rpm). After 5 min of reaction, the mixed samples were heated at high temperature (100 °C) to stop the digestion. Subsequently, obtained mixture was centrifuged (3500 rpm, 4 ℃) for 10 min, and the protein concentration was also measured (biuret method). MPN flexibility was assessed as follows:

$$MPN\ flexibility\ (\%/min) = \frac{C_i - C_m}{5 \times C_i} \times 100 \quad (4)$$

Where C_i and C_m are the initial protein concentration and the measured protein content, respectively.

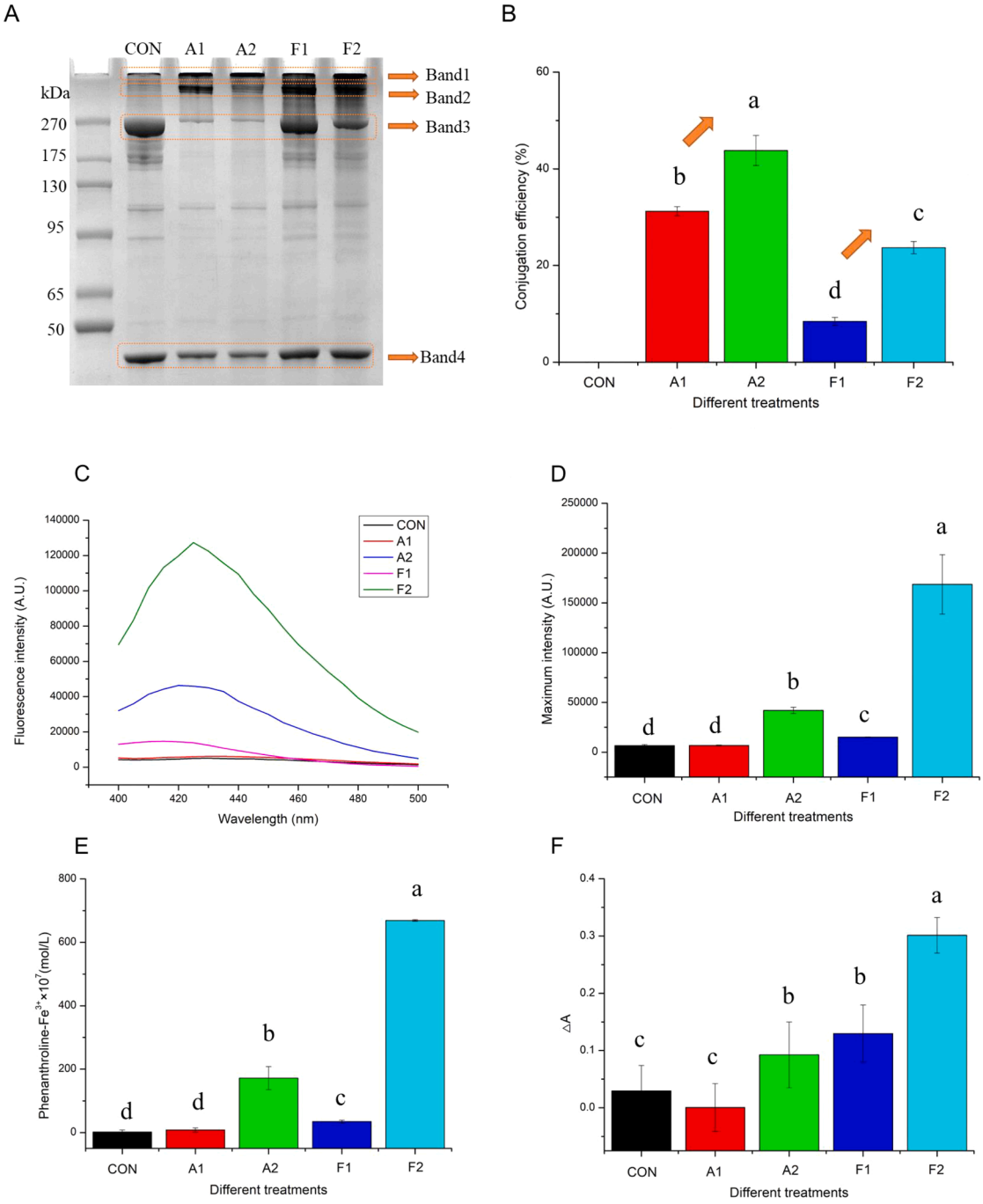

Fig. 1. Protein pattern by (A) SDS-PAGE of chicken MPN as affected by covalent grafting and UDT (band 3: myosin heavy chain). Impact of the UDT upon various modifications (alkaline reaction and free radical oxidation) on the (B) conjugation efficiency of GA on MPN. Effects of different covalent reactions and added UDT on the free radical contents of the systems through terephthalic acid (C-D), phenanthroline (E) and crystal violet (F) dosimetry. Values with different letters (a − e) in (B, D, E and F) indicate significantly different (p <.05).

2.15. Statistical analysis

The data were presented in the form of mean ± standard deviation. Statistical significances of these data were analyzed by SAS software. Significant differences among means (CON, A1, A2, F1 and F2) were measured through one-way analysis of variance (ANOVA, $p < .05$). Difference groups were also evaluated through Tukey's multiple comparisons.

3. Results and discussion

3.1. Synthesis of MPN-GA polymers

Alkaline reaction and free radical oxidation have been proven as efficient methods for the formation of MPN–GA polymers. In Fig. 1, two obvious polymers (band 1 and 2) were observed in the A1 and A2 groups. Moreover, the density of identified myosin heavy chain (band 3) decreased after the grafting. These changes indicated that GA quinone generated in alkaline environment reacted with some active residues [9] in MPNs, contributing to the formation of MPN cross-links (MPN–N–GA–N–MPN and/or MPN–S–GA–S–MPN). Similar trends were also observed in the F1 and F2 groups. It was understandable since amino acids in the MPN chains tended to be oxidized by the ascorbate radicals produced in the ascorbic acid/hydrogen peroxide system [21]. In this regard, these radicals localized on MPN further reacted with GA through newly formed covalent bonds. In contrast to free radical oxidation, a more obvious change in myosin heavy chain (band 3) was achieved in Fig. 1. This result showed that MPNs were easier to form protein cross-linking under alkaline conditions. Our results were inconsistent with previous studies. It was reported [22] that more active sites were available to interact with polyphenols in the free radical oxidation. However, Liu et al. [23] concluded that the synthesis of phenolic–protein conjugates was highly correlated with the nature of protein. Additionally, diverse reaction times might also lead to the differences between our results and those reported studies.

Notably, the relatively lower density of myosin heavy chain (band 3) in the F2 group than in the F1 group were probably attributable to the strengthening effect of UDT. During free radical oxidation, UDT promoted the structural transformation of MPN via the strong cavitation effect, contributing to the protein cross-linking. Liu et al. [2] also reported that the destruction of the filamentous protein structure after UDT (150–600 W, 15 min, 20 kHz, 20 °C) provided additional binding sites. Unfortunately, this advantage was not observed in alkaline reactions. This can be ascribed to the fact that a relatively higher cross-linking degree of myosin in the MPN has already been induced under the conventional alkaline condition (A1). At this time, the crosslinking process cannot be further enhanced by UDT. Our previous study [9] concluded that UDT-triggered radicals were helpful to the generation of low molecular weight MPN fragments (350 W/L, 6 min, 4 °C). Pan et al. [6] reported that the improved effect of UDT (400 W, 10 min, 20 kHz, 10 °C) on protein cross-linking was connected with the dose of GA. Furthermore, the strengthening effect of UDT could also be ascribed to the actual intensity [24] of the treatments.

In view of the shortcoming of SDS-PAGE, total GA contents and conjugation efficiency were evaluated. As summarized, the GA contents were 4.69, 6.57, 1.27 and 3.55 μmol/g in the A1, A2, F1 and F2 after modifications, respectively. This result revealed that GA was successfully grafted on MPN molecules. It was noteworthy that conjugation efficiency increased by 12.57% and 15.25%, respectively, at strengthening system of alkaline reaction (A2) and free radical oxidation (F2) when compared with their original groups (A1 and F1). UDT often exhibits excellent impacts on decreasing the aggregation level of various proteins via using their turbulent forces, such as fish MPN (400 W, 10 min, 20 kHz, 10 °C), bovine serum albumin (500 W, 0–30 min, 20 kHz, 0–4 °C), and β-casein (500 W, 0–30 min, 20 kHz, 0–4 °C) [6,25]. In this regard, the dynamic reaction equilibrium proceeds in a direction that is conducive to the formation of MPN-GA conjugates. Previous study of Li et al. [7] demonstrated that the transformation of protein conformation during UDT (100–300 W, 40 min, 20 kHz, 70 °C) also resulted in the production of more conjugates. Interestingly, the change of conjugation efficiency in F2 was more markedly evident (from 8.44 ± 0.85% to 23.69 ± 1.26%) when compared with that in A2 (from 31.24 ± 0.93 % to 43.81 ± 3.12%). This could be explained by the limited reactive sites of MPN available for further reactions under the alkaline environment [26]. As aforementioned, a relatively high cross-linking degree of MPN was not conducive to the further covalent grafting of GA during the strengthening effect of UDT. It was therefore concluded that MPNs were easily modified by UDT in the free radical oxidation system. Besides, extra OH· generated by UDT can also affect the covalent reaction of MPN, which will be discussed in the following chapters.

3.2. Free radical contents

Free radical contents of different reactions were measured through terephthalic acid, phenanthroline and crystal violet dosimetry. The result implied that the application of UDT into the system did not decrease the production of final OH·, but on the contrary did accelerate the generation of phenanthroline-Fe^{3+} and 2-hydroxyterephthalic acid. A previous study [6] also confirmed the important role of free radicals triggered by UDT in the oxidation. Furthermore, the lifting effects of the final products in the F2 group was more pronounced than that in the A2 group, indicating that more OH· was generated during UDT-assisted free radical reaction. In this regard, the presence of hydrogen peroxide in the F2 group caused additional dissociation [27] under the action of UDT (formula 5–8), thereby enhancing the formation of OH· and hence higher rise rate of conjugation efficiency. This also evidenced that the maximum degree of intensification was achieved by the combination of UDT and free radical oxidation.

$$H_2O + UDT \rightarrow OH\cdot + H\cdot \quad (5)$$

$$H_2O_2 + UDT \rightarrow 2OH\cdot \quad (6)$$

$$UDT \rightarrow h^+ + e^- \quad (7)$$

$$H_2O_2 + e^- + H^+ \rightarrow H_2O + OH\cdot \quad (8)$$

Generally, a stronger disruption effect can be obtained when coupled with physical forces of UDT if the concentration of OH· in the liquid is higher [10]. Additionally, free radicals are highly transient, and their yields are closely related to the environment. To simplify discussion, this study discussed using the OH· as free radicals in strengthening pathways only (ascorbate radicals in the free radical oxidation was ignored). In this work, the strengthening effect of the chemical part depended on the free radicals provided by UDT. These free radicals could be acquired by two pathways. First, the water molecule was firstly dissociated ($H_2O \rightarrow OH\cdot + H\cdot$) by ultrasonic cavitation, resulting in the generation of OH· [28], subsequently attacking the MPNs and GA to form the conjugates. Due to the structure changes of GA induced by OH· during UDT, MPN cross-linking could be strengthened [6]. Furthermore, the production of radicals was associated with the properties of cavitation bubbles in the medium [10]. Clearly, a relatively high cross-linking degree of MPN in the A2 group may be detrimental to the role of OH· in cavitation bubbles. This will be further discussed in the viscosity properties part. The second way referred to the extra generation of free radicals in the presence of hydrogen peroxide [19,23]. It is important to note that the OH· in this way can only be obtained in the group F2. As a result, a more obvious grafting change rate was acquired in the free radical oxidation.

3.3. Particle sizes and ζ-potential

Particle size distribution and D[4,3] values were shown in Fig. 2. Noticeably, a broad peak at 100 μm was achieved in particle size curves

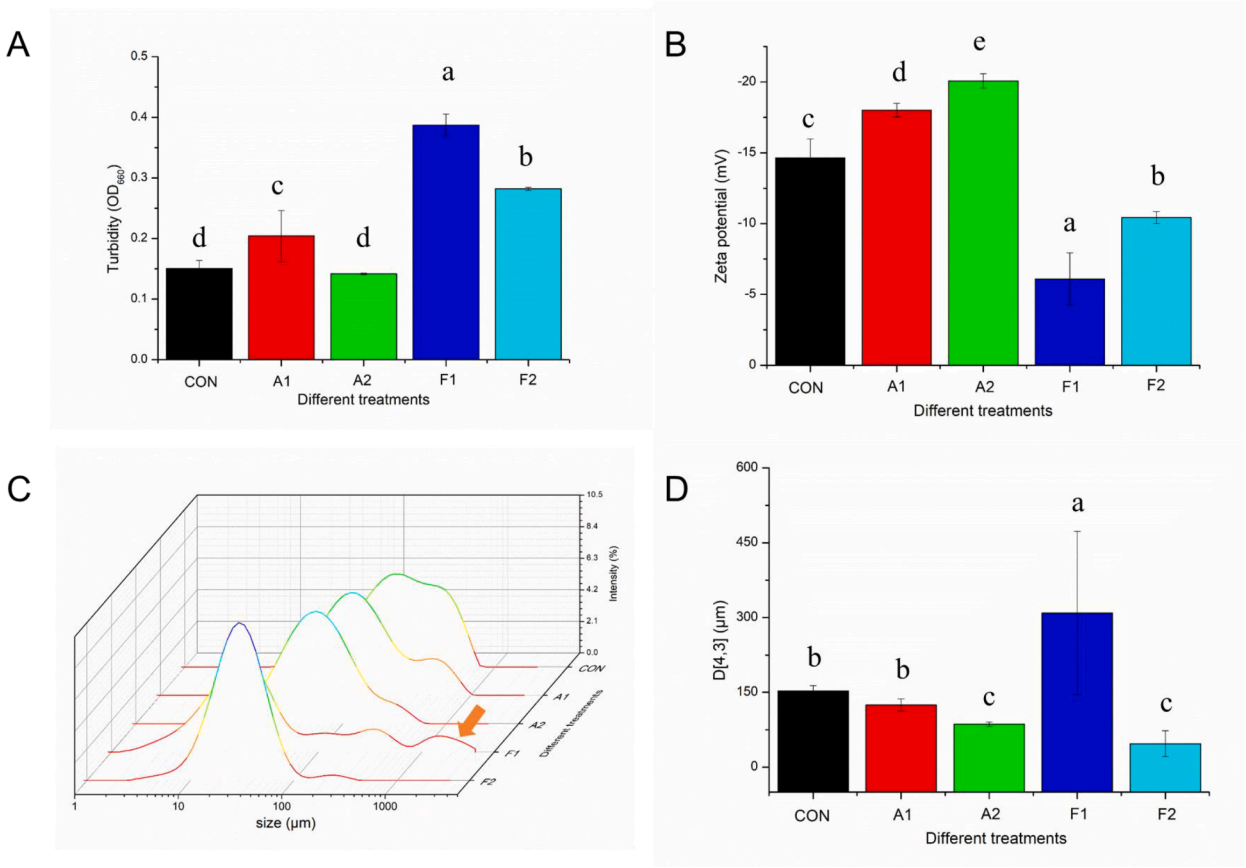

Fig. 2. Effects of different covalent reactions (alkaline reaction and free radical oxidation) and added UDT on (A) turbidity value, (B) ζ-potential, (C) particle size distribution and (D) D [4,3] value of MPNs. Values with different letters (a – e) in (A, B, and D) indicate significantly different (p <.05).

of all groups. Moreover, another new peaks of the F1 group could be observed in the larger size number (about 1000 μm), indicating that some irregular MPN-GA aggregates were formed after conventional free radical oxidation. A certain number of hydroxyl groups in GA [19] could form hydrogen bonds with amino groups in MPN side chains. At the same time, OH· attacked the MPN chain, leading to the formation of covalent bonds between GA and protein. These covalent and non-covalent interactions caused the protein aggregation to shift toward higher particle sizes. In the UDT-assisted oxidation system, due to the application of UDT, these peaks dissociated into small particle size distribution in the F2 group. UDT damaged non-covalent interactions between MPN molecules through the strong agitation (150–600 W, 15 min, 20 kHz, 0–20 °C) [29], allowing these aggregates previously formed in the molecules to be destroyed. The decrease of particle size was also reported in other proteins, such as beef protein, soy protein isolate and rapeseed protein [30–31]. UDT exhibited the ability to effectively destroy hydrogen bond and electrostatic force of plant proteins (50 W/L, 10 min, 20 kHz, 40 °C) [32]. By comparison, meat proteins, especially MPNs, are more sensitive [33]. Furthermore, the area of filamentous meat proteins that can be cavitated is larger than that of whey protein particles [2].

These acquired data were further evaluated through D[4,3] values. The D[4,3] decreased by 30.80% and 84.74%, respectively, at UDT-assisted oxidation groups of alkaline reaction (A2) and free radical grafting (F2) when compared with their natural groups (A1 and F1). UDT treatment has been recognized [2] as an useful and green method to disarrange the ordered structure of experimental protein, resulting in a noticeably reduction in the D[4,3] values of MPN. Moreover, initial myofilament structure of MPN might be dissociated after the action of violent physical cavitation force produced by UDT. In this regard, myosin and/or actin were released, accompanied by the protein unfolding, leading to the decrease in D[4,3] values. Another studies [14,33] also attributed this change to the breakdown of chemical bonds in protein. Interestingly, no significant difference was achieved in D [4,3] between the A2 group and the F2 group, showing that UDT disrupted the original agglomerates and masses in free radical oxidation (F1). This, in turn, verified that stronger cavitation bubble effects in the free radical oxidation, which was in line with the discussion in section 3.2.

The ζ-potential was applied to assess the depression and aggregation of MPNs. Amiri et al. [30] mentioned that MPNs with high absolute values changed the protein aggregation, as well as promoting the dispersion of MPN. Our results also indicated that whereas the alkaline reaction enhanced the surface charge (absolute value) of MPN, free radical oxidation decreased this tendency, thereby disturbing the MPN aggregation. The differences between the A1 group and the F1 group could be ascribed to the reaction principle and properties of these conjugates [23]. Interestingly, the lowest ζ-potential intensity (negative charge) was achieved in the A2 group subjected to the UDT, indicating that MPN particles were stabilized by the strongest electrostatic repulsion [29]. Besides, this transformation was also tightly associated with the accessibility of MPN polar residues on their surface [2]. It was noticed that the increasing rate of ζ-potential intensity of the F2 group (71.32%) was much higher than that of the A2 group (11.48%) after UDT, indicating that more polar residues were available on MPN surface after being treated by the sonication. Larger ζ-potential change in the F2 group could also be attributed to the stronger binding ability of GA (negative charges) to MPN under the free radical oxidation. Our previous discussion pointed out that more OH· produced at this time (the F2 group) contributed to the grafting reaction of MPN. Chen et al. [11]

attributed the ζ-potential changes to 'stress response' and unfolding structure during UDT. Likewise, Liu et al. reported that the assembly of fibrous protein was inhibited by the additional electrostatic repulsion [2], resulting in the improvement of the MPN stability. Extra action of cavitation bubbles and free radicals in the UDT-assisted free radical oxidation might destroy the natural structure of MPNs, thereby the looser conformation was obtained owing to the negative charges distributed on the MPN surface. Consequently, the combination of UDT and free radical oxidation was more effective due to the stronger action at this time.

3.4. SEH and SLT

SEH was applied as an essential indicator for assessing the unfolding degree of MPN. As reported [34], it reflected the amounts of exposed hydrophobic binding cavities on MPN. As shown in Fig. 3, SEH content of protein decreased from 28646.48 to 20773.33 and 25285.56 after alkaline reaction and free radical oxidation, respectively. As subjected to the UDT, two groups (A2 and F2) exhibited significantly upward trends, whose measured fluorescence intensities were 52500.93 and 58792.96, respectively. These results implied that conventional oxidation treatments inhibited the exposure of hydrophobic groups. In addition, the crosslinking structure formed during the oxidation hindered the partial unfolding of protein, making original hydrophobic groups buried in the interior regions hard to be exposed. However, noticeable enhancement in SEH contents were observed by Huang et al. [35] when they investigated the oxidation reaction between mulberry polyphenols and beef MPN. Furthermore, Zhou et al. [36] reported that the addition of quercetin also increased the SEH of MPN, thereby improving the cooking quality of cured meat. A potential explanation for the differences in SEH changes could be the various properties of experimental polyphenols. More so, protein state and polyphenol contents may also affect the MPN unfolding state.

The noteworthy point is that the SEH value of MPN was enhanced substantially after UDT. Additionally, the increasing rate of SEH intensity of the F2 group (183.02%) was significantly higher than that of the A2 group (83.27%) after the sonication, implying that extra action of cavitation bubbles and free radicals in the F2 group promoted the migration of the MPN hydrophobic groups. Conformational stretching and/or partial unfolding of protein were responsible for leading to a sensitive state [11] of MPN during the UDT. Meanwhile, these proteins could not return to their original state. In this regard, slight increase of free radical contents and repeated action of cavitation bubbles strengthened the denaturation of MPN structure. Thus, a relatively higher rate of SEH enhancement was found in the F2 group. A previous study [30] reported that most hydrophobic amino acids were negatively charged. Also, the increase of these SEH values in MPN samples improved the electrostatic repulsions between MPN chains, contributing to the stability of the system. As supported by the ζ-potential results, a stronger interaction in the F2 group was obtained. Pan et al. [6] also believed that the alteration of protein SEH was closely connected with the amount of GA. The best synergistic effect of UDT and GA on the SEH of MPN could be obtained at 400 W, 5 min and 25 μmol/g. Another study [37] reported that this changes maybe result from the different resistances of the conjugation containing quercetin and whey protein to UDT.

In Fig. 3, SLT of the control group was 176.38 μmol/100 mg protein. In general, GA formed their corresponding quinone structure under alkaline condition, which could further reacted with –SH in MPN, leading to the decrease in SLT. However, a slight enhancement of SLT was observed in the A1 group (195.47 μmol/100 mg). This result can be explained by the protein unfolding process during the experiment.

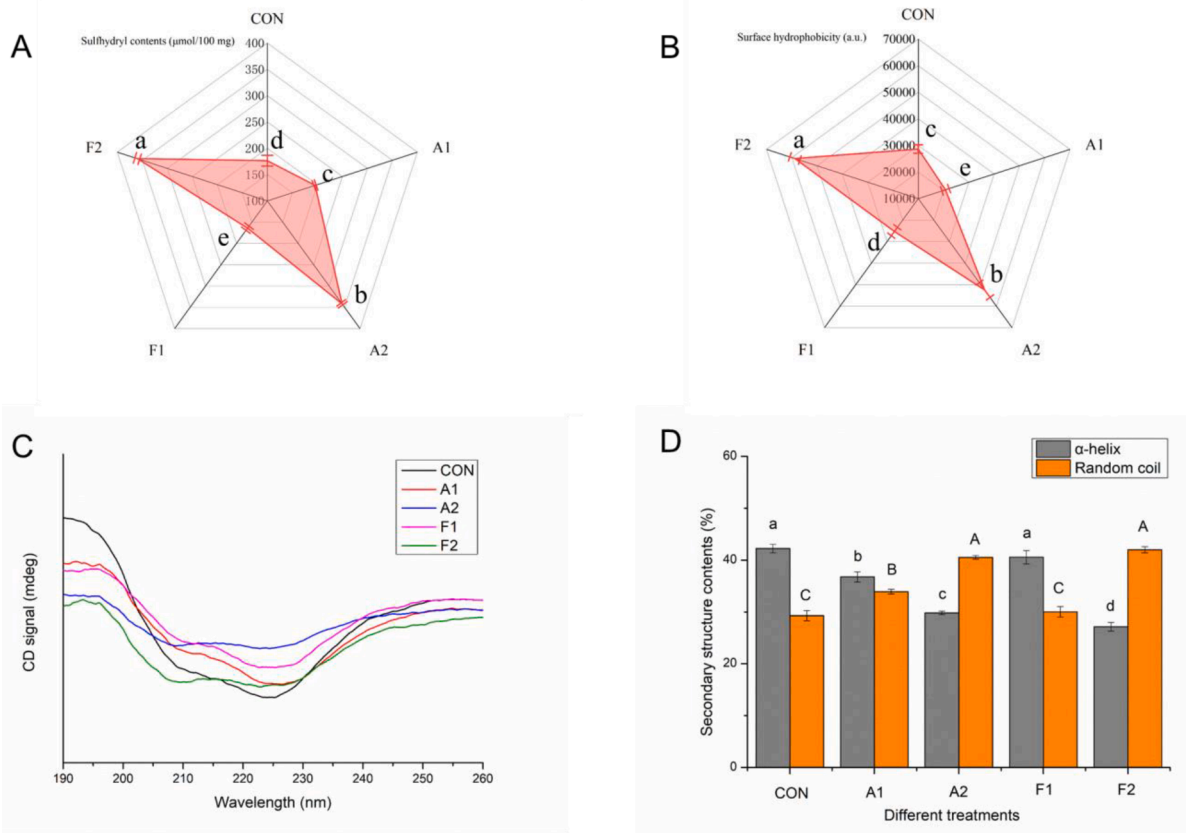

Fig. 3. Effects of different covalent reactions (alkaline reaction and free radical oxidation) and added UDT on (A) SLT and (B) SEH of MPNs. (C) Circular dichroism spectra and (D) secondary structure information of MPNs following different treatments. (E) Steady-state shear and (F) transient shear properties of MPNs as affected by covalent reactions and UDT. Values with different letters (a – e) in (A, B, and D) indicate significantly different ($p < .05$).

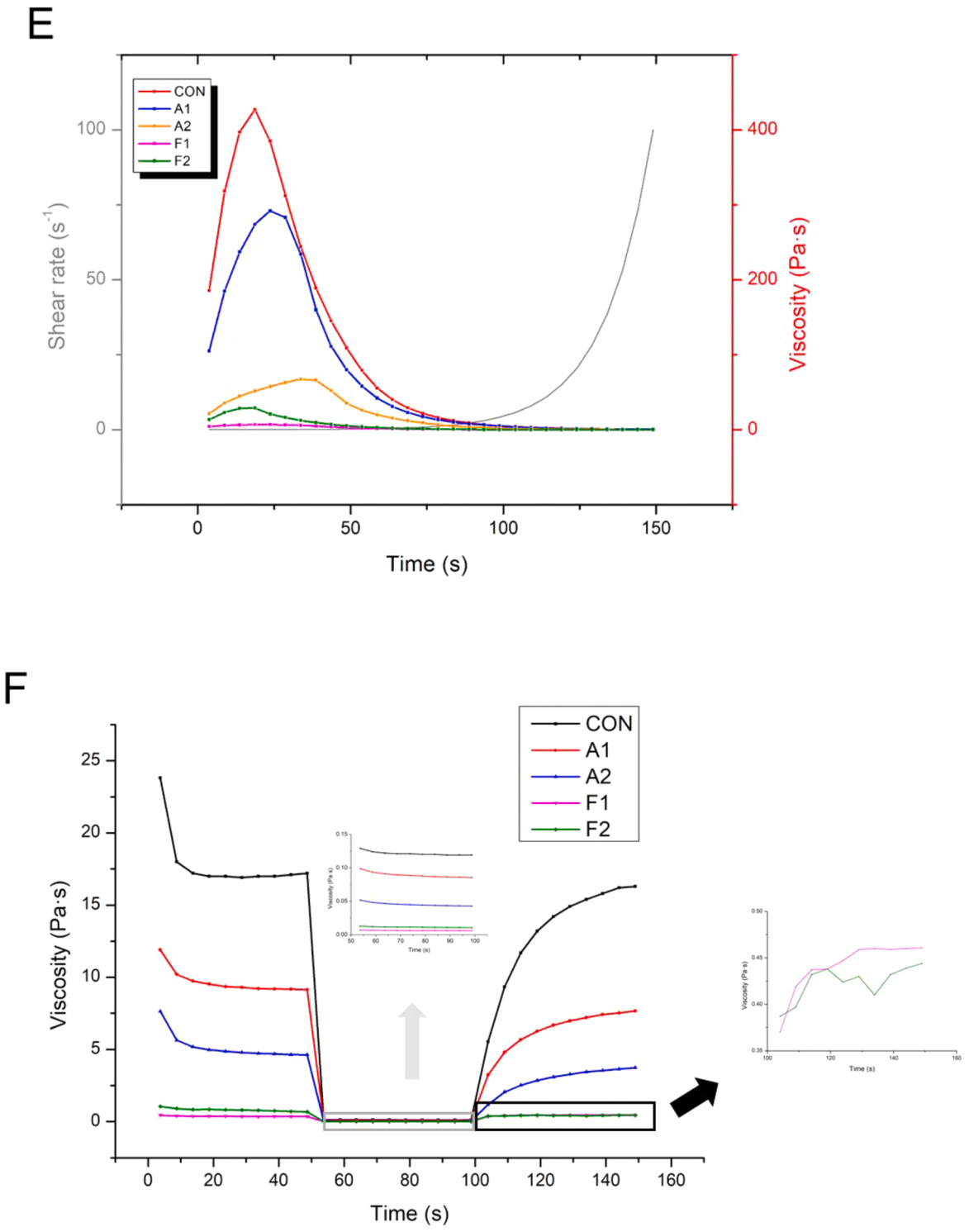

Fig. 3. (*continued*).

Before the alkaline reaction, the system was adjusted to a pH of 9.0. At this time, a certain amount of sulfhydryl groups were exposed to the MPN surface, accompanied by the expansion of MPN compact structure [32]. After the reaction, the system was readjusted back to a pH of 7.0. However, these exposed SLT groups were not buried during this refolding process, resulting in the increase of final SLTs. This may be related to the hydrogen bonds between exposed SLT groups and polyphenols [38]. To note, this explanation was further confirmed in the neutral pH oxidation group. Obviously, SLT of the F1 group decreased from 176.38 to 164.13 μmol/100 mg (the control group), corresponding to the consumption of sulfhydryl groups in the covalent reaction. Notably, the SLT change rates of alkaline reaction and free radical oxidation were 74.86% and 119.38% after the UDT, respectively. It was implied that UDT-assisted free radical oxidation group (F2) promoted a more intense MPN unfolding. Amiri et al. [14] reported that the majority of these buried active groups were unmasked via disrupting the natural MPN structure after the UDT. In addition, another study [32] concluded that changes in protein size also accelerated the transformation of SLT groups. In conclusion, a stronger cavitation effect in the free radical oxidation system boosted the SLT changes when compared with alkaline

system.

3.5. Secondary structure

While SEH and SLT measurements showed the unfolding state of treated proteins, the secondary structure of various MPNs was also evaluated to further investigate more about the conformational changes after modifications. The circular dichroism spectra of different MPNs exhibited two obvious peaks at 209 and 226 nm (Fig. 3), corresponding to their natural α-helix structure. As can be seen, the magnitudes of these bands of the CON group were destroyed after covalently binding with GA, indicating that ordered MPN structures were disrupted and/or lost. According to the obtained results, the α-helix contents were decreased apparently by 12.94% and 3.98% for the A1 ($p < .05$) and F1 group ($p > .05$), respectively. The α-helix structure might be dissociated during the pH changes of the alkaline reaction. This finding was in agreement with that reported by Li et al. [15], since pH-shifting treatment increased the misfolding degree of chicken MPN. Moreover, this result can also be explained by more severe MPN crosslinking in the A1 group than in the F1 group (section 3.1). Another study [39] also suggested that the interaction between phenolic hydroxyl groups of polyphenol and proteins might also change the α-helix structure of MPN.

In regard to the UDT-assisted oxidation groups, the sonication further decreased the α-helix proportions of experimental conjugates, corresponding to 29.83% and 27.17%, respectively, in the A2 and F2 group. Needless to say, UDT broke hydrogen interactions [11] in MPN-GA, converting compact α-helix into random coil. It could also be attributed to the fact that the UDT disrupted the MPN strands [30], thereby promoting the expansion of protein structure. In contrast, UDT-assisted alkaline reaction group (A2, 29.36%) showed a higher percentage of decline than that of UDT-assisted radical grafting system (F2, 35.67%). This may be linked with the stronger synergistic effect between UDT and free radical oxidation. Another report [19] also suggested that the partially unfolding state and loose structure of the MPN was intensely beneficial to the covalent reaction of protein and polyphenol. At this time, the increased OH· was more conductive to the improvement of conjugation efficiency in the UDT-assisted free radical oxidation.

3.6. Turbidity

The turbidity testing of various MPN solutions after modifications was shown in Fig. 2, which was widely studied to reflect the protein molecules aggregation state [40]. It has been proven [41] that the greater turbidity value represented poor MPN distribution. All the conventional oxidation treatments markedly increased the turbidity value, followed by a significantly downward trend when the UDT was introduced. It can be attributed to the fact that newly formed protein crosslinks after the covalent reactions interfered light scattering, thereby increasing the turbidity. Additionally, exposed hydrophobic residues on MPN are prone to aggregate via hydrophobic interaction. Meanwhile, the sample turbidity significantly decreased after the UDT. This may be because the high-intensity physical effect [33] of UDT inhibited the potential of MPN aggregation. Also, protein dissolution behavior [41] during UDT was obviously beneficial to the decrease of turbidity. Unexpectedly, the proportion of turbidity reduction of the UDT-assisted alkaline reaction group (30.61%) was marginally higher than that of UDT-assisted radical grafting system (27.16%). A potential explanation for the results may be the fact that covalent grafting [9] of phenolic compounds on proteins contributes to the browning reactions of experimental conjugates. Yan et al. [42] also reported the unique color changes in the alkaline reaction.

3.7. Viscosity properties

3.7.1. Steady-state shear properties

The steady-state shear properties of various MPN and MPN-GA systems (CON, A1, A2, F1 and F2) are depicted in Fig. 3. Generally, the apparent viscosity changes of the systems are essential to reflecting the molecular transformation and physicochemical properties of proteins. As can be seen, similar shear-thinning behaviors of all protein samples were achieved as the shear rate increasing from 0.01 s^{-1} to 100 s^{-1}. These viscosity results indicated the typical non-Newtonian characteristics of different MPN systems. Previous literature [14] also reported similar viscosity properties of meat MPNs. Moreover, apparent viscosities of CON, A1, A2, F1 and F2 at 0.01 s^{-1} were 186, 105, 21.4, 4.29 and 13.3 Pa·s, respectively. It seems that UDT caused completely different effects on the viscosities of these two different systems. Our previous study [9] pointed out that UDT could increase the viscosity of MPN at 100 s^{-1} through rearranging the protein molecules. However, Amiri et al. concluded [14] that strong forces of UDT destroyed stable chemical bonds in MPNs, leading to the decrease of the sample fluidity. These differences of viscosity change after UDT may be closely related to the intensity of acoustic cavitation, protein state and experimental environment.

As designed, Power law model (final fitting degree $\geq$ 0.99) and Carreau model (final fitting degree $\geq$ 0.91) were applied in this part to further assess the viscosity properties of different MPNs. Consistency parameter (k) of MPNs in the power law model was linked with conjugate-conjugate interactions and pseudoplastic behaviors in the system. As summarized (Table 1), lower k values were observed in the A1 (14.37 Pa·s^n) and F1 (0.58 Pa·s^n) group. It is considered that covalent reaction destroyed internal frictions among MPN-GAs. Similar weaker protein interactions were reported by Li et al. [15]. The results showed that UDT decreased the k value of the A1 group (from 14.37 Pa·s^n to 7.26 Pa·s^n), while the F1 group performed a strengthening trend (from 0.58 Pa·s^n to 0.90 Pa·s^n). A postulation was that UDT enhanced the protein crosslinks in the free radical oxidation, insinuating an intensive increase in consistency. Meanwhile, a higher protein crosslinks has been already achieved in the A1 group. At this time, consistency cannot be further enhanced by UDT [43] in the alkaline reaction. It was also supported that modified protein state [44] and steric hindrance after different covalent reactions might also cause the differences in UDT effects.

Zero shear viscosity (η_0) in Carreau model provides more information about the effects of different reactions on the initial MPNs structure. Our previous study [9] also concluded that the alternation of breaking speed and winding speed in this work led to the destruction of original complex structure of MPNs. All of η_0 values decreased significantly, which indicated the weak entanglement state of MPN suspensions after modifications. Also, two notable decreases in the A1 and F1 group (Table 1) referred to a more thinner system due to the regulations of covalent reactions. Compared with non-UDT-treated group after free radical oxidation, MPNs treated with UDT showed higher η_0 values, which reflected the more chain frictions. However, the η_0 values of

Table 1
GA contents, rheological parameters (k and η_0) and protein flexibility of MPNs after different treatments (CON, A1, A2, F1 and F2).

Treatments	CON	A1	A2	F1	F2
GA contents (μmol/g)	—	4.69 ± 0.14^{b}	6.57 ± 0.47^{a}	1.27 ± 0.13^{d}	3.55 ± 0.19^{c}
k (Pa·s^n)	18.94 ± 0.60^{a}	14.37 ± 0.56^{b}	7.26 ± 0.23^{c}	0.58 ± 0.02^{e}	0.90 ± 0.02^{d}
η_0 (Pa·s)	483.58 ± 74.86^{a}	309.67 ± 45.72^{b}	61.53 ± 5.34^{c}	7.22 ± 0.44^{e}	35.05 ± 4.17^{d}
MPN flexibility (%/min)	0.99 ± 0.34^{c}	0.66 ± 0.36^{c}	1.42 ± 0.43^{ab}	1.08 ± 0.16^{bc}	1.52 ± 0.43^{a}

Note: Different letters (a-e) indicated significant differences.

alkaline oxidation-treated group decreased obviously after UDT, accounting for the serious destroying of the rod-shaped chain structure of MPNs. These changes further confirmed the difference of acoustic cavitation in the process of free radical oxidation and alkaline oxidation.

It was also found that the important factor affecting the action effect of acoustic cavitation [10] is the viscosity of the experimental solution. It can be predicted that the increase of protein viscosity hindered the generation of cavitation bubbles because of the low oscillating effects in the medium. The higher viscosity of the A1 group revealed that alkaline oxidation allowed harder diffusion of cavitation bubbles. In comparison, evident decrease in viscosity led to a stronger strengthening effect in the F2 group. Therefore, the distinctive synergy of the F2 group cannot be simply ascribed to the additional degradation of hydrogen peroxide during UDT. Taken together, it was proposed that both viscosity properties and extra OH· in the free radical oxidation improved the potential of UDT to enhance the covalent reactions.

3.7.2. Transient shear properties

Viscosities of various MPN and MPN-GA systems (CON, A1, A2, F1 and F2) under high-speed (400 s^{-1}) and low-speed shear rate (1 s^{-1}) were also measured (Fig. 3F). In early trials (0–50 s), the viscosity of modified protein suspension decreased in the order of CON > A1 > A2 > F2 > F1. As experimental time increased, the viscosity values also decreased for both conventional oxidation groups and UDT-assisted groups. The main reason for decreasing viscosity [45] in this shear rate range may be the rearrangement of MPN-GA. Furthermore, non-covalent interactions [14] between negatively charged MPNs also had an impact on the final viscosity of the system. These non-covalent interactions might be broken down by high-speed (400 s^{-1}) shear rate. Evidently, all groups showed a decrease trend when the shear rate changed from 1 s^{-1} to 400 s^{-1}. With the increasing experimental time (100–150 s), the viscosities of MPN and MPN-GA systems gradually increased. It can be attributed to the production of MPN-MPN (or MPN-GA-MPN-GA) aggregates during the high-to-low-speed (from 400 s^{-1} to 1 s^{-1}) shearing process. Besides, non-covalent interactions increased again under the low-speed (400 s^{-1}) shear rate. Notably, there was no obvious difference ($p > .05$) in the viscosity for the free radical oxidized samples (F1 and F2) in the third period. This further verified the low degree of protein crosslinking in the process of free radical oxidation. Results were consistent with those of protein gel electrophoresis.

Based on these results, we concluded that MPNs with a relatively low viscosity exhibited excellent responses during the action of cavitation bubbles. As going through covalent reactions of MPN, natural structures of these proteins were easier to be modified by enhanced acoustic cavitation. As a consequence, the contents of GA bound to MPN were improved. Hence, antioxidant properties, microstructure and protein flexibility of MPNs after various treatments (CON, A1, A2, F1 and F2) were subsequently evaluated.

3.8. Antioxidant properties

The antioxidant activities of MPN-GA conjugate after different GA modifications (CON, A1, A2, F1 and F2) were systematically investigated through DPPH, ABTS and ion reduction capacities (Fig. 4). Obviously, all MPN-GA samples (0.01–4 mg/mL) showed sufficient DPPH scavenging capacities. At a relatively higher concentration (4 mg/mL), the DPPH scavenging capacities of CON, A1, A2, F1 and F2 were 15.22%, 71.83%, 80.32%, 45.86%, and 59.18%, respectively. Similar antioxidant activities of MPNs after covalent binding with GA were also reported by Xu et al.[19]. Besides, the ABTS and ion reduction capacities of MPN-GA samples (A1, A2, F1 and F2) were apparently higher than those of MPN group (CON). Above results demonstrated that the GA grafting on MPNs tremendously enhanced the original antioxidant activities of protein. Notably, the proportion of changes in DPPH scavenging capacities of the UDT-assisted alkaline reaction system (29.24%) was obviously higher than those of UDT-assisted radical grafting system

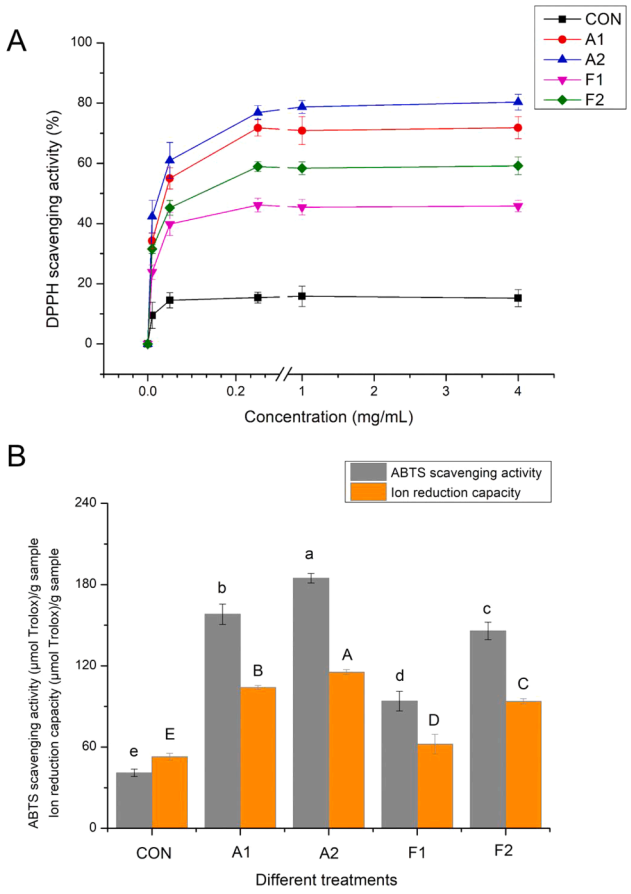

Fig. 4. Effects of different covalent reactions (alkaline reaction and free radical oxidation) and added UDT on (A) DPPH scavenging activities, (B) ABTS scavenging activities and ion reduction capacities of MPNs. Values with different letters (a − e or A-E) in (B) indicate significantly different ($p < .05$).

(11.82%) at an equivalent concentration. Similarly, the increasing rates of ABTS and ion reduction capacities of the F2 group (ABTS: 55.16%, ion reduction: 50.98%) was significantly higher than those of the A2 group (ABTS: 16.82%, ion reduction: 10.98%), showing that UDP induced better antioxidant activities in free radical oxidations.

These results were consistent with the improvement of conjugate efficiency in in section 3.1. Chen et al. [46] studied the antioxidant activities of protein–polyphenol conjugates, they finally connected these properties with the concentration of oxidized polyphenols. Our previous study [9] believed that the antioxidant properties of polyphenols-MPN conjugates were closely related to the strength of the synergistic effect produced by UDT and covalent reaction. It is well established that more active sites were available on MPN after being influenced by the forceful sonication [6], leading to the improvement of antioxidant activities when compared with non-UDT-treated groups (A1 and F1). In our work, the low-viscosity environment of the free radical oxidation system resulted in the stronger cavitation, promoting the covalent binding with GA and final antioxidant properties. Additionally, a more clear enhancement of antioxidant activity in the F2 group could also be ascribed to their significantly structural changes, which were in agreement with previous results. In summary, the combination of UDT and free radical oxidation was more effective for improving the antioxidant activities because of the best synergistic action.

3.9. Microstructure

The microstructure of various MPN and MPN-GA systems (CON, A1, A2, F1 and F2) was evaluated by AFME (Fig. 5). MPN in the CON group

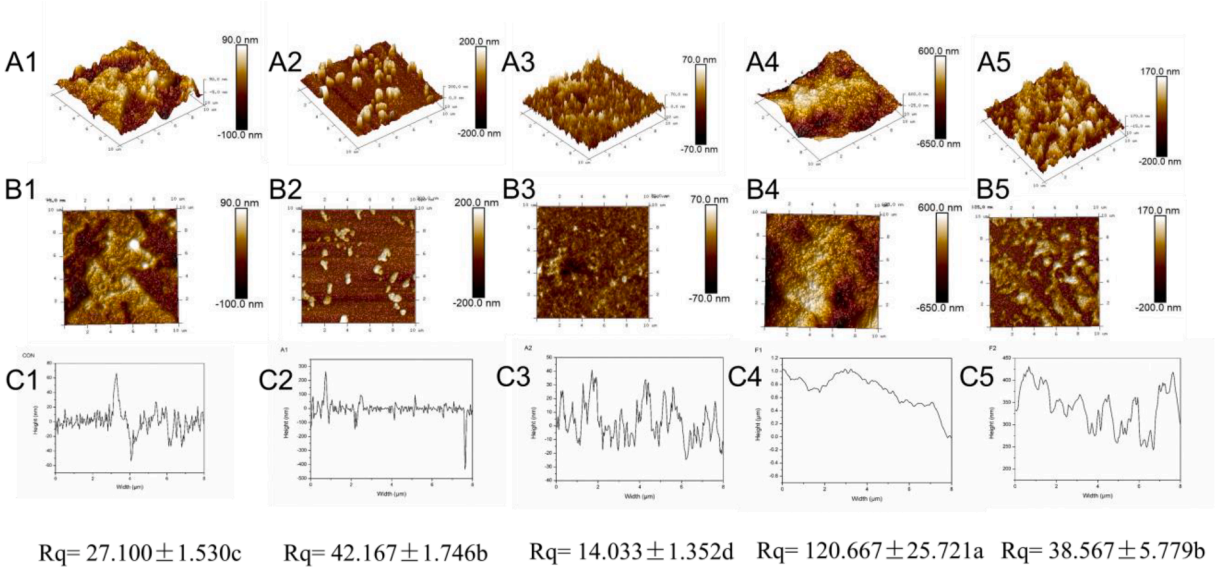

Fig. 5. Effects of different covalent reactions (alkaline reaction and free radical oxidation) and added UDT on (A1-A5) 3D images, (B1-B5) 2D images, (C1-C5) cross-sections, Rq values of MPNs. Values with different letters (a − d) in the figure indicate significantly different (p <.05).

exhibited aggregated fibrous distribution. With the application of alkaline reaction, MPNs appeared to display as irregular spherical particles (A1). However, these accumulated fibrous structures were retained after the free radical oxidation (F1). Interestingly, all MPN-GA systems began to show a well-distributed fibrous structure after the UDT (A2 and F2). Additionally, the cross-sections (height distribution) and Rq were effectively influenced by UDT. It illustrated that the roughness and inhomogeneity of the system were reduced by acoustic cavitation. Liu et al. [2] found that the stable filamentous structure of MPN were changed when proteins were subjected to UDT. Li et al. [15] also linked this microstructure change with their loose structure. It was assumed that sharp change of MPN morphology under alkaline reaction led to an inert state of proteins. Hence, it was hard for cavitation bubbles to act on the proteins due to the transformation in their shapes. In comparison, the retention of fibrous structure under free radical oxidation was more susceptible to acoustic cavitation than the spherical shape [47]. It certificated that the slight change of MPNs microstructure resulting from free radical oxidation contributed to a notable improvement on acoustic cavitation effects.

3.10. MPN flexibility

The protein flexibility is usually recognized as a distinctive property for reflecting MPN function. In this situation, MPNs with higher molecular flexibility are more likely to change their spatial structure as the surrounding environment changes. The MPN flexibility of the A1 group was slightly lower than that of the CON group, but the measured value after free radical oxidation was marginally higher for the F1 group. The more cross-linked protein structure after grafting suggested a lower molecular structure flexibility of MPNs, resulting in a reduction in flexibility value. In contrast to the UDT-assisted free radical oxidation in the F2 group, the MPN flexibility treated with UDT and alkaline reaction increased more significantly. It seemed to be contrary to our previous discussion that UDT-assisted free radical oxidation displayed a better synergy. Actually, protein flexibility [48,49] is highly connected with their hierarchical structures. As confirmed in the microstructure, a relatively lower change of fibrous structure in free radical oxidation suggested a smaller protein flexibility at this time. Even though there was almost no change in the fibrous structure of MPN after UDT-assisted free radical oxidation, it was more sensitive than the spherical structure in the alkaline reaction. It was reasonable to speculate that the retention of MPN fibrous structure improved the action effects of acoustic cavitation.

3.11. Proposed molecular mechanism of different systems

The key mechanism of the synergistic effect of UDT and covalent reactions on MPNs was explained by chemical (acoustic cavitation radical) and physical effect (acoustic mechanical action). In the present work, the stronger improvements in the combination of UDT and free radical oxidation (F2) were discussed by the following deductions (Fig. 6): 1) the UDT promoted the additional decomposition of hydrogen peroxide in the F2 group, increasing the contents of OH· and final oxidation effects. 2) Furthermore, the distinctive synergy of the F2 group cannot be simply attributed to the additional generation of OH·. The decrease of protein viscosity in the free radical oxidation also speed up the generation of cavitation bubbles due to the high oscillating effects during the UDT. 3) the retention of fibrous structure under free radical oxidation was more susceptible to acoustic cavitation than the spherical shape formed in the alkaline reaction.

4. Conclusions

This work successfully verified that the synergistic effect of UDT and free radical oxidation was better than alkaline reaction. It was found that UDT-assisted reactions promoted the stronger changes of conjugate efficiency, structural and physicochemical properties of MPN. UDT triggered the exposure of more SEH and SLT during the covalent reactions. Notably, the secondary structure of MPN were modified by both UDT and covalent reactions, of which the proportions of α-helix decreased but random coil increased. Moreover, the advantages from UDT-assisted free radical oxidation were also proven by more drastic rate of particle sizes and ζ-potential change of the MPN-GA. Simultaneously, higher increasing rate of antioxidant properties of UDT-assisted free radical oxidation were also found. It should be noticed that the relatively low viscosity, retained fibrous structure and additional OH· in the free radical oxidation jointly accelerated the maximization of synergy. This study explained the potential mechanisms of MPN changes induced by UDT-assisted covalent reactions, which aims to seek the better synergistic action to maximize process efficiency.

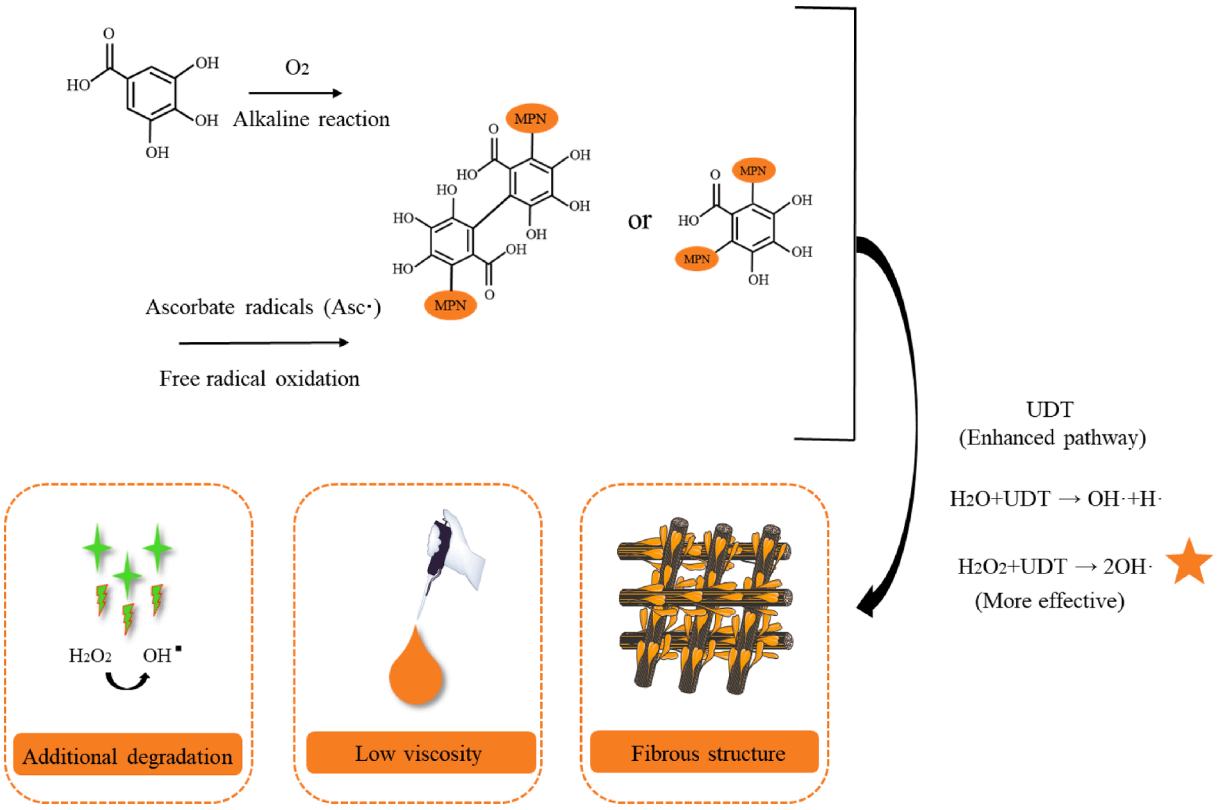

Fig. 6. Schematic mechanism of the UDT impact on covalent reactions of MPNs.

CRediT authorship contribution statement

Jiahui Chen: Conceptualization, Methodology, Data curation, Writing – original draft. **Xing Chen:** Methodology, Conceptualization. **Guanghong Zhou:** Supervision, Funding acquisition. **Xinglian Xu:** Writing – review & editing, Supervision, Funding acquisition.

Declaration of Competing Interest

The authors declare that they have no known competing financial interests or personal relationships that could have appeared to influence the work reported in this paper.

Acknowledgments

This work was supported by the National Natural Science Foundation of China (No. 31972097), China Agriculture Research System of MOF and MARA (CARS-41), and a project funded by the Priority Academic Program Development of Jiangsu Higher Education Institution (PAPD).

References

[1] A.D. Alarcon-Rojo, L.M. Carrillo-Lopez, R. Reyes-Villagrana, M. Huerta-Jiménez, I. A. Garcia-Galicia, Ultrasound and meat quality: A review, Ultrason. Sonochem. 55 (2019) 369–382.
[2] H. Liu, H. Zhang, Q. Liu, Q. Chen, B. Kong, Solubilization and stable dispersion of myofibrillar proteins in water through the destruction and inhibition of the assembly of filaments using high-intensity ultrasound, Ultrason. Sonochem. 67 (2020), 105160.
[3] H. Liu, Z. Wang, I.H. Badar, Q. Liu, Q. Chen, B. Kong, Combination of high-intensity ultrasound and hydrogen peroxide treatment suppresses thermal aggregation behaviour of myofibrillar protein in water, Food Chem. 367 (2022), 130756.
[4] O. Karimi-Khouzani, E. Heidarian, S.A. Amini, Anti-inflammatory and ameliorative effects of gallic acid on fluoxetine-induced oxidative stress and liver damage in rats, Pharmacol. Rep. 69 (2017) 830–835.
[5] Y.-C. Chia, R. Rajbanshi, C. Calhoun, R.H. Chiu, Anti-neoplastic effects of gallic acid, a major component of Toona sinensis leaf extract, on oral squamous carcinoma cells, Molecules 15 (2010) 8377–8389.
[6] J. Pan, H. Lian, H. Jia, S. Li, R. Hao, Y. Wang, X. Zhang, X. Dong, Ultrasound treatment modified the functional mode of gallic acid on properties of fish myofibrillar protein, Food Chem. 320 (2020), 126637.
[7] Z. Li, Y. Zheng, Q. Sun, J. Wang, B. Zheng, Z. Guo, Structural characteristics and emulsifying properties of myofibrillar protein-dextran conjugates induced by ultrasound Maillard reaction, Ultrason. Sonochem. 72 (2021), 105458.
[8] L.M. Carrillo-Lopez, M. Huerta-Jimenez, I.A. Garcia-Galicia, A.D. Alarcon-Rojo, Bacterial control and structural and physicochemical modification of bovine Longissimus dorsi by ultrasound, Ultrason. Sonochem. 58 (2019), 104608.
[9] J. Chen, X. Zhang, M. Fu, X. Chen, B.A. Pius, X. Xu, Ultrasound-assisted covalent reaction of myofibrillar protein: The improvement of functional properties and its potential mechanism, Ultrason. Sonochem. 76 (2021), 105652.
[10] S. Krishnan, N.A. Ghani, N.F. Aminuddin, K.S. Quraishi, B. L. Razafindramangarafara, S. Baup, J.-M. Leveque, Unexpected acceleration of Ultrasonic-Assisted iodide dosimetry in the catalytic presence of ionic liquids, Ultrason. Sonochem. 74 (2021), 105576.
[11] J. Chen, X. Zhang, Y. Chen, X. Zhao, B. Anthony, X. Xu, Effects of different ultrasound frequencies on the structure, rheological and functional properties of myosin: Significance of quorum sensing, Ultrason. Sonochem. 69 (2020), 105268.
[12] K. Slinkard, V.L. Singleton, Total phenol analysis: automation and comparison with manual methods, Am. J. Enol. Viticult. 28 (1977) 49–55.
[13] S. Koda, T. Kimura, T. Kondo, H. Mitome, A standard method to calibrate sonochemical efficiency of an individual reaction system, Ultrason. Sonochem. 10 (2003) 149–156.
[14] A. Amiri, P. Sharifian, N. Soltanizadeh, Application of ultrasound treatment for improving the physicochemical, functional and rheological properties of myofibrillar proteins, Int. J. Biol. Macromol. 111 (2018) 139–147.
[15] L. Li, X. Zhao, X. Xu, Trace the difference driven by unfolding-refolding pathway of myofibrillar protein: Emphasizing the changes on structural and emulsion properties, Food Chem. 367 (2022), 130688.
[16] V. Tirtaatmadja, D. Boger, J. Fraser, The dynamic and steady shear properties of synovial fluid and of the components making up synovial fluid, Rheol. Acta 23 (1984) 311–321.
[17] J. Zhang, X. Hou, H. Ahmad, H. Zhang, L. Zhang, T. Wang, Assessment of free radicals scavenging activity of seven natural pigments and protective effects in AAPH-challenged chicken erythrocytes, Food Chem. 145 (2014) 57–65.
[18] A. Yıldırım, A. Mavi, A.A. Kara, Determination of antioxidant and antimicrobial activities of Rumex crispus L. extracts, J. Agr. Food Chem. 49 (2001) 4083–4089.
[19] Y. Xu, M. Han, M. Huang, X. Xu, Enhanced heat stability and antioxidant activity of myofibrillar protein-dextran conjugate by the covalent adduction of polyphenols, Food Chem. 352 (2021), 129376.

[20] K.S. Kim, C. Woodward, Protein internal flexibility and global stability: effect of urea on hydrogen exchange rates of bovine pancreatic trypsin inhibitor, Biochemistry-US 32 (1993) 9609–9613.
[21] F. Liu, C. Sun, W. Yang, F. Yuan, Y. Gao, Structural characterization and functional evaluation of lactoferrin–polyphenol conjugates formed by free-radical graft copolymerization, RSC Adv. 5 (2015) 15641–15651.
[22] J. You, Y. Luo, J. Wu, Conjugation of ovotransferrin with catechin shows improved antioxidant activity, J. Agr. Food Chem. 62 (2014) 2581–2587.
[23] J. Liu, H. Yong, X. Yao, H. Hu, D. Yun, L. Xiao, Recent advances in phenolic–protein conjugates: Synthesis, characterization, biological activities and potential applications, RSC Adv. 9 (2019) 35825–35840.
[24] X. Deng, Y. Ma, Y. Lei, X. Zhu, L. Zhang, L. Hu, S. Lu, X. Guo, J. Zhang, Ultrasonic structural modification of myofibrillar proteins from Coregonus peled improves emulsification properties, Ultrason. Sonochem. 76 (2021), 105659.
[25] D. Xu, L. Li, Y. Wu, X. Zhang, M. Wu, Y. Li, Z. Gai, B. Li, D. Zhao, C. Li, Influence of ultrasound pretreatment on the subsequent glycation of dietary proteins, Ultrason. Sonochem. 63 (2020), 104910.
[26] K. Chen, X. Chen, L. Liang, X. Xu, Gallic acid-aided cross-linking of myofibrillar protein fabricated soluble aggregates for enhanced thermal stability and a tunable colloidal state, J. Agr. Food Chem. 68 (2020) 11535–11544.
[27] S.K. Gujar, P.R. Gogate, Application of hybrid oxidative processes based on cavitation for the treatment of commercial dye industry effluents, Ultrason. Sonochem. 75 (2021), 105586.
[28] Z.D. Xue, Q.A. Zhang, H.R. Zheng, Roles of free radical on the formation of acetaldehyde in model wine solutions under different ultrasound parameters: A key bridge-link compound for red wine coloration during ageing, Ultrason. Sonochem. 79 (2021), 105757.
[29] H. Liu, J. Zhang, H. Wang, Q. Chen, B. Kong, High-intensity ultrasound improves the physical stability of myofibrillar protein emulsion at low ionic strength by destroying and suppressing myosin molecular assembly, Ultrason. Sonochem. 74 (2021), 105554.
[30] A. Amiri, P. Sharifian, N. Morakabati, A. Mousakhani-Ganjeh, M. Mirtaheri, A. Nilghaz, Y.-G. Guo, A. Pratap-Singh, Modification of functional, rheological and structural characteristics of myofibrillar proteins by high-intensity ultrasonic and papain treatment, Innov. Food Sci. Emerg. 72 (2021), 102748.
[31] N. Wang, X. Zhou, W. Wang, L. Wang, L. Jiang, T. Liu, D. Yu, Effect of high intensity ultrasound on the structure and solubility of soy protein isolate-pectin complex, Ultrason. Sonochem. 80 (2021), 105808.
[32] Y. Li, Y. Cheng, Z. Zhang, Y. Wang, B.K. Mintah, M. Dabbour, H. Jiang, R. He, H. Ma, Modification of rapeseed protein by ultrasound-assisted pH shift treatment: Ultrasonic mode and frequency screening, changes in protein solubility and structural characteristics, Ultrason. Sonochem. 69 (2020), 105240.
[33] J. Chen, X. Zhang, S. Xue, X. Xu, Effects of ultrasound frequency mode on myofibrillar protein structure and emulsifying properties, Int. J. Biol. Macromol. 163 (2020) 1768–1779.
[34] C. Zhang, X.-A. Li, H. Wang, X. Xia, B. Kong, Ultrasound-assisted immersion freezing reduces the structure and gel property deterioration of myofibrillar protein from chicken breast, Ultrason. Sonochem. 67 (2020), 105137.
[35] X. Huang, L. Sun, L. Liu, G. Wang, P. Luo, D. Tang, Q. Huang, Study on the mechanism of mulberry polyphenols inhibiting oxidation of beef myofibrillar protein, Food Chem. 372 (2022), 131241.
[36] Z.Q. Zhou, Q.D. Xu, L. Chen, N. Chen, H.X. Gao, Q. Sun, W.C. Zeng, Interaction and action mechanism of quercetin and myofibrillar protein and its effects on the quality of cured meat, J. Food Process. Pres. (2021), e16020.
[37] W.N. Baba, R. Abdelrahman, S. Maqsood, Conjoint application of ultrasonication and redox pair mediated free radical method enhances the functional and bioactive properties of camel whey-quercetin conjugates, Ultrason. Sonochem. 79 (2021), 105784.
[38] J. Chen, Y. Xu, B.A. Pius, P. Wang, X. Xu, Changes of myofibrillar protein structure improved the stability and distribution of baicalein in emulsion, LWT-Food Sci. Technol. 137 (2021), 110404.
[39] J. Cheng, M. Zhu, X. Liu, Insight into the conformational and functional properties of myofibrillar protein modified by mulberry polyphenols, Food Chem. 308 (2020), 125592.
[40] T. Gill, J. Chan, K. Phonchareon, A. Paulson, Effect of salt concentration and temperature on heat-induced aggregation and gelation of fish myosin, Food Res. Int. 25 (1992) 333–341.
[41] S. Jiang, D. Zhao, Y. Nian, J. Wu, M. Zhang, Q. Li, C. Li, Ultrasonic treatment increased functional properties and in vitro digestion of actomyosin complex during meat storage, Food Chem. 352 (2021), 129398.
[42] X. Yan, Y. Gao, S. Liu, G. Zhang, J. Zhao, D. Cheng, Z. Zeng, X. Gong, P. Yu, D. Gong, Covalent modification by phenolic extract improves the structural properties and antioxidant activities of the protein isolate from Cinnamomum camphora seed kernel, Food Chem. 352 (2021), 129377.
[43] Y.-Y. Wang, M.T. Rashid, J.-K. Yan, H. Ma, Effect of multi-frequency ultrasound thawing on the structure and rheological properties of myofibrillar proteins from small yellow croaker, Ultrason. Sonochem. 70 (2021), 105352.
[44] A. Amiri, A. Mousakhani-Ganjeh, S. Shafiekhani, R. Mandal, A.P. Singh, R. E. Kenari, Effect of high voltage electrostatic field thawing on the functional and physicochemical properties of myofibrillar proteins, Innov. Food Sci. Emerg. 56 (2019), 102191.
[45] N. Zhao, H. Zou, S. Sun, C. Yu, The interaction between sodium alginate and myofibrillar proteins: The rheological and emulsifying properties of their mixture, Int. J. Biol. Macromol. 161 (2020) 1545–1551.
[46] Y. Chen, S. Jiang, Q. Chen, Q. Liu, B. Kong, Antioxidant activities and emulsifying properties of porcine plasma protein hydrolysates modified by oxidized tannic acid and oxidized chlorogenic acid, Process Biochem. 79 (2019) 105–113.
[47] L. Xu, Y. Zheng, C. Zhou, D. Pan, F. Geng, J. Cao, Q. Xia, Kinetic response of conformational variation of duck liver globular protein to ultrasonic stimulation and its impact on the binding behavior of n-alkenals, LWT-Food Sci. Technol. 150 (2021), 111890.
[48] C.H. Tang, L. Shen, Role of conformational flexibility in the emulsifying properties of bovine serum albumin, J. Agr. Food Chem. 61 (2013) 3097–3110.
[49] J. Du, C. Zhou, Q. Xia, Y. Wang, F. Geng, J. He, Y. Sun, D. Pan, J. Cao, The effect of fibrin on rheological behavior, gelling properties and microstructure of myofibrillar proteins, LWT-Food Sci. Technol. 153 (2022), 112457.